Journal of Materials Chemistry B

ROYAL SOCIETY OF CHEMISTRY

PAPER

View Article Online
View Journal | View Issue

Cite this: J. Mater. Chem. B, 2022, 10, 3895

Passerini chemistries for synthesis of polymer pro-drug and polymersome drug delivery nanoparticles†

Alessandra Travanut,[a] Patrícia F. Monteiro,[a] Sean Smith,[b] Steven M. Howdle,[b] Anna M. Grabowska,[c] Barrie Kellam,[a] Michael A. R. Meier[d] and Cameron Alexander *[a]

Received 7th January 2022,
Accepted 16th April 2022

DOI: 10.1039/d2tb00045h

rsc.li/materials-b

New materials chemistries are urgently needed to overcome the limitations of existing biomedical materials in terms of preparation, functionality and versatility, and also in regards to their compatibility with biological environments. Here, we show that Passerini reactions are especially suited for the preparation of drug delivery materials, as with relatively few steps, polymers can be synthesized with functionality installed enabling drug conjugation and encapsulation, self-assembly into micellar or vesicular architectures, and with facile attachment triggerable chemistries. The polymers can be made with a variety of building blocks and assemble into nanoparticles, which are rapidly internalized in triple negative breast cancer (TNBC) cells. In addition, the polymers transport drug molecules efficiently through 3D cell cultures, and when designed with chemistries allowing pH-mediated release, exhibit greater efficacy against TNBC cells compared to the parent drug.

Introduction

Polymers for therapeutic delivery are required to meet stringent criteria,[1,2] including diverse functionalities to allow attachment and/or encapsulation of drugs and targeting agents, an intrinsically degradable backbone, and should be synthetically accessible in as few steps as possible.[3,4] In addition, for systemic administration, it is advantageous if the polymers can assemble into nanoscale particles with a hydrophilic exterior, in order to circulate in the bloodstream and avoid early excretion.[5–7] However, most existing polymer drug delivery systems in the clinic are derived from a relatively small range of lactides, glycolides and lactones.[8] These chemistries are sub-optimal in terms of the ultimate function of biomedical polymer structures, with problems of poor compatibility with candidate drug compounds and low functional group content without complex and costly synthesis. In addition, for formulations that are administered systemically, the existing stock of materials are difficult to modify to alter their rate of biodegradation.[9] In recent years, the Passerini multicomponent reaction (Passerini-MCR), which combines a carboxylic acid, an aldehyde and an isocyanide into a α-acyloxycarboxamide product in a straightforward and atom economic procedure,[10–12] is emerging as an alternative route to biomedical materials. The Passerini reaction has been widely investigated in organic chemistry, but also offers a powerful route to functional polymers, as it can provide in a single step the synthesis of complex, multifunctional and highly defined macromolecular architectures.[13] Passerini reactions also bring important advantages from a translational pharmaceutical perspective.[14] These include facile and scalable chemistry, the potential for multiple functionalities (*e.g.* hydrogen bonding, or reactive linkers) in one structure from one reaction, easy routes to varied polymer architectures[15] and predictable degradation under various biological conditions.[16–18] In turn, these factors enable tuning of drug compatibility, extent of drug loading or encapsulation, and modulation of biodistribution. The intrinsic biodegradability of the Passerini ester-amide product (α-acyloxycarboxamides) extends the utility of this reaction for many further applications beyond drug delivery. We have previously shown a simple approach for the Passerini-MCR synthesis of a new biodegradable amphiphilic diblock copolymer, which self-assembled into vesicles that were well-tolerated by numerous cell lines and long-circulating *in vivo*.[13] Here, we exploit the Passerini-MCR functionality to deliver an anti-cancer drug by two different routes from the same inherent polymer materials

[a] School of Pharmacy University of Nottingham, Nottingham NG7RD, UK. E-mail: Cameron.alexander@nottingham.ac.uk
[b] School of Chemistry University of Nottingham, Nottingham NG7RD, UK
[c] School of Medicine, University of Nottingham, Nottingham NG7RD, UK
[d] Karlsruhe Institute of Technology, Institute of Organic Chemistry (IOC) and Institute of Biological and Chemical Systems, Functional Molecular Systems (IBCS-FMS), Straße am Forum 7, Building 30.48 76131, Karlsruhe, Germany. E-mail: m.a.r.meier@kit.edu

† Electronic supplementary information (ESI) available. See DOI: https://doi.org/10.1039/d2tb00045h

platform. In the first example, we use the self-assembly properties of the Passerini polymer amphiphile to form polymersomes, which can be used to encapsulate the drug for a more sustained release profile. In the second case, we utilize the high functional group content in the polyester–polyamide backbone to conjugate the anticancer drug *via* a pH-responsive linker for enhanced intracellular release. We chose to exemplify this approach with doxorubicin, which is one of the mainstay treatments for TNBC, an aggressive subtype of breast cancer and a leading cause of cancer deaths.[19] TNBC is characterized by the absence of human epidermal growth factor receptor 2 and the lack of progesterone and estrogen receptors,[20,21] it also affects young patients and those in certain population groups, and has high metastatic potential. Unfortunately, TNBC has poor clinical outcomes,[22] with only 30–40% of chemotherapy-treated patients in early stage TNBC showing positive responses to therapies.[23] Doxorubicin as a free drug has severe side-effects including dose-limiting cardiotoxicity, and hence the encapsulation of doxorubicin in a number of carriers has been carried out as a way to enhance therapeutic index. Liposomal doxorubicin is used successfully to treat a number of cancers, but for TNBC, in which combination therapies are typically employed, there is a need for carrier materials which might be amenable to both drug encapsulation and drug conjugation strategies. Here we have employed Passerini chemistries to explore both routes for doxorubicin delivery, and report the results of *in vitro* efficacy studies with TNBC cells in both 2D and 3D culture.

Materials and methods

Materials

The following chemicals were used as received: trimethyl orthoformate (≥99%, Aldrich), thionyl chloride (≥97%, Aldrich), diisopropylamine (≥99%, Aldrich), phosphorus(V) oxidychloride (≥99%, Aldrich), 10-undecenal (≥90%, Aldrich), 3-mercaptopropionic acid (≥99%, Aldrich), 2-2-dimethoxy-2-phenylacetophenone (DMPA, (≥99%, Aldrich), *tert*-butyl isocyanide (98%, Aldrich), *O*-methyl-*O*′-succinylpolyethylene glycol 2′000 (Aldrich), triethylamine (≥99%, Aldrich), 3-buten-1-ol (≥98%, Aldrich), dimethyl sulfide (≥99%, Aldrich), *N*,*N*′-dicyclohexylcarbodiimide (99%, Aldrich), *N*-hydroxysuccinimide (≥97%, Aldrich), 1,5,7-triazabicyclo[4.4.0]dec-5-ene (Aldrich),4-(Dimethylamino)pyridine (≥99%, Aldrich), silica gel 60 (0.035–0.070, Aldrich), chloroform-d ($CDCl_3$, 99.96% D, 0.03% v/v TMS, Aldrich), deuterium oxide (99.9% D, Aldrich), Triton X-100 (Aldrich), Sephadex® LH20, phosphate buffered saline (PBS) (Dulbecco's, Aldrich). TrypLE™ Express Enzyme (1X) no phenol red (GibcoTM), Hoechst 33342, CellMask™ Green plasma membrane stain was purchased from Thermo Fisher Scientific. Cyanine5 (**Cy5**) ammine fluorescent dye was purchased from Lumiprobe. CellTiter-Fluor™ Cell Viability Assay (Promega, Madison WI), L-glutamine (Aldrich), RPMI-1640 media and fetal bovine serum (FBS) were obtained from Life Technologies (Carlsbad, CA, USA). All solvents used were of technical grade.

Measurements

Thin-layer chromatography (TLC) identification of reactants and products was performed on silica-gel-coated aluminum foil (Aldrich, silica gel 60, F 254 with fluorescence indicator). Compounds were visualized by permanganate stain solution (mixture of potassium permanganate, potassium carbonate and sodium hydroxide in water).

Nuclear Magnetic Resonance (NMR) spectra were recorded using a Bruker DPX400 UltraShield™ Spectrometer at 400 MHz (^{1}H) and 101 MHz (^{13}C). All ^{1}H NMR spectra were reported in ppm relative to the solvent signal for chloroform-*d* at 7.26 ppm. All ^{13}C NMR spectra were reported in ppm relative to the central line of the triplet for chloroform-d at 77.16 ppm. The spectra produced were analysed with MestReNova 12.0.4 (Mestrelab Research S.L.).

ESI-TOF Mass Spectrometry measurements were carried out with ESI† positive ionization mode using a Bruker microTOFII mass spectrometer employed with flow injection sample induction with electrospray ionization (ESI).

Size exclusion chromatography (SEC) was performed on an Agilent 1260 infinity series HPLC with an online vacuum degasser, an Agilent online differential refractometer (DRI) and a Wyatt Heleos II Multi-Angle Light Scattering detector (MALS). Two Agilent 5 μm PLgel Mixed E columns (7.5 × 300 mm) were connected in series with an Agilent PLgel 5 μm guard column (7.5 × 50 mm). The column oven, DRI and MALS temperature were set to 35 °C and the flow rate was set to 1 mL per minute. Each sample was dissolved in HPLC grade tetrahydrofuran (THF), at a concentration of 1 mg mL^{-1}. DRI calibration was performed using 30 kDa and 200 kDa linear polystyrene narrow dispersity standards dissolved in THF at a concentration of 1.0 mg mL^{-1}.

Particle size measurements were recorded using a Malvern Zetasizer Nano Series (Malvern, UK) instrument supported by Zetasizer Software 7.11, where all the measurements were carried out at a scattering angle of 90° and a temperature of 25 °C and the results were recorded as average of 10 runs ± SD.

Transmission electron microscopy. Polymersome morphologies were analysed on a Tecnai G2 (FEI, Oregon USA) transmission electron microscope (TEM) and the samples were stained using a solution of uranyl acetate 2% in water.

Confocal microscopy and flow cytometry analyses. Cells were imaged with a Zeiss LSM 700 Confocal Laser Scanning Microscope. Zen 2.6 blue image Software was utilized for image processing.

Flow cytometry analyses were performed on Coulter FC-500 cytometer (Beckman Coulter) and Kaluza Analysis 2.1 software was used to perform the analyses. Absorbance and fluorescence readings of cells in 96 well plates were performed by using a TECAN Spark 10 M plate reader.

Synthetic procedures

Synthesis of 12-methoxy-12-oxododecan-1-aminium chloride (1). 12-Aminododecanoic acid (4.31 g, 18.75 mmol) was suspended in 50 mL of methanol. The suspension was cooled in an

ice bath and subsequently 4.21 mL of thionyl chloride (6.9 g, 58.12 mmol) was added dropwise at 0 °C. After addition of thionyl chloride, the solution was warmed to room temperature and stirred overnight. The solution was then poured into 350 mL of diethyl ether and stored in the freezer overnight. The product was then filtered off and dried under high vacuum. The product 12-methoxy-12-oxododecan-1-aminium **(1)** was obtained as a white solid, yield 80% (3.45 g, 15 mmol). ESI-MS of $[C_{13}H_{28}NO_2]^+$ (M^+) = calc. 230.21 found 230.21.

Synthesis of methyl 12-formamidododecanoate (2). 12-Methoxy-12-oxododecan-1-aminium chloride **(1)** (3.31 g, 14.3 mmol) was dissolved in 29 mL of trimethyl orthoformate (28.1 g, 0.143 mol) and heated to 100 °C for 12 h. Trimethyl orthoformate was removed under reduced pressure and methyl 12-formamidododecanoate **(2)** was used without any further purification.

Synthesis of methyl 12-isocyanododecanoate (3). Methyl 12-formamidododecanoate **(2)** (3.67 g, 14.3 mmol) was dissolved in 77 mL dichloromethane (0.34 M) and 6.21 mL diisopropylamine (4.48 g, 44.3 mmol) was added, the reaction mixture was cooled to 0 °C. Subsequently, 1.763 mL phosphorous oxychloride (2.85 g, 18 mmol) was added dropwise and the reaction mixture was then stirred at room temperature for 2 h. The reaction was quenched by addition of sodium carbonate solution (20%, 48 mL) at 0 °C. After stirring this mixture for 30 minutes, 52 mL water and 52 mL dichloromethane were added. The aqueous phase was separated and the organic layer was washed with brine (4 × 32 mL). The combined organic layers were dried over sodium sulphate and the solvent was evaporated under reduced pressure. The crude product was then purified by column chromatography (hexane/EtOAc 100% : 0% to 80% : 20%). Methyl 12-isocyanododecanoate **(3)** was collected as a yellow oil 2.79 g, 11.5 mmol, yield 80.4% – R_f: 0.34 EtOAc 20% – hexane 80%.

^{13}C NMR (101 MHz, $CDCl_3$) δ 174.30 C_h, 155.71 C_m, 51.46 C_g, 41.66 C_a, 34.12 C_f, 29.44-29.15 C_d, 28.72 C_b, 26.35 C_e, 24.97 C_c.

ESI-MS of $[C_{14}H_{25}NO_2]$ $(M+Na)^+$ = calc. 262.19 found 262.17.

Synthesis of but-3-en-1-yl 12-isocyanododecanoate (4). The synthesis was adapted from a prior method.[24] Methyl 12-isocyanododecanoate **(3)** (0.512 g, 2.14 mmol) and 1,5,7-triazabicyclo[4.4.0]dec-5-ene (TBD) (0.059 g, 0.4 mmol) were dissolved in 0.5 mL of dichloromethane (DCM), then 3-buten-1-ol (0.77 g, 10.7 mmol) was added. The reaction was stirred at RT for 1 h and then heated to 40 °C at 280 mbar for 10 h under rotary evaporation. The crude product was diluted with 2 mL of DCM and the TBD was partially precipitated in cold diethyl ether. The supernatant was washed with water two times, the organic phase was dried over magnesium sulfate, filtered and dried under rotary evaporation. But-3-en-1-yl 12-isocyanododecanoate **(4)** was collected as a colorless oil (0.261 g, 0.9 mmol, yield 43.8%).

^{1}H NMR (400 MHz, CDCl3) δ/ppm: δ 5.87 (dd, 1H, J = 16.9, 10.1, 6.8 Hz, CH_b), 5.09 (dt, 2H, J = 19.9, 10.1 Hz, CH_a), 4.10 (t, 2H, J = 6.7 Hz, CH_d), 3.39–3.30 (m, 2H, CH_n), 2.42–2.21 (m, 4H, CH_{ce}), 1.75–1.56 (m, 4H, CH_{mf}), 1.40 (dd, 2H, J = 14.2, 6.8 Hz, CH_h), 1.26 (s,12H, CH_g).

^{13}C NMR (101 MHz, CDCl3) δ 173.86 Cp, 155.38 Co, 134.96 Cb, 117.26 Ca, 63.25 Cd, 41.60 Cn, 34.27 Ce, 33.08 Cc, 29.37–29.18 Cg, 28.65 Ch, 26.27 Cf, 24.92 Cm ESI-MS of [C17H29NO2] $(M + H)^+$ = calc. 280.22 found 280.22; $(M + Na)^+$ = calc. 302.22 found 302.20.

Synthesis of AB-type monomer (5)

10-Undecenal (1.71 g, 10.0 mmol) and DMPA (134 mg, 0.50 mmol) were placed in a quartz tube and dissolved in 4.0 mL of tetrahydrofuran (THF). Then, the tube was purged with argon for 10 min and afterward the solution was exposed to UV light (365 nm) for 30 s. Subsequently, 3-mercaptopropionic acid (1.17 g, 11.0 mmol) was slowly added. The reaction mixture was stirred for 2 h under UV irradiation. Then, the solvent was evaporated under reduced pressure and the crude product was purified by silica gel column chromatography (*n*-hexane/ethyl acetate = 3 : 1–1 : 1) to yield a white solid (1.78 g, 65%). R_f = 0.30 (dichloromethane/methanol = 20 : 1).

^{1}H NMR (400 MHz, CDCl3) δ/ppm: δ 9.76 (s, 1H, CH_a), 2.80-2.75 (t, 2H, J = 6.2 Hz, CH_h) 2.70–2.61 (t, 2H, J = 6.2 Hz, CH_i), 2.61–2.46 (m, 2H, CH_g), 2.42–2.39 (m, 2H, CH_c) 1.67–1.55 (m, 4H, CH_{df}), 1.35–1.27 (m, 12H, CH_e).

^{13}C NMR (101 MHz, CDCl3) δ 203.24 C_a, 177.49 C_n, 44.04 C_c, 34.74 C_g, 32.34 C_i, 29.64 C_f, 29.45, 29.27–28.94 C_g, 26.77 C_d, 22.21 C_h.

ESI-MS of $[C_{14}H_{26}O_3S]$ $(M-H)^-$ = calc. 273.16 found 273.15; $(M + H)^+$ = calc. 275.16 found 275.16; $(M + Na)^+$ = calc. 297.14 found 297.09.

Synthesis of P1 – Passerini-3CR polymerization

The synthesis was adapted from a previous route.[13] To a vigorously stirred solution of *O*-methyl-*O*′-succinyl polyethylene glycol 2 kDa (0.25 g, 0.118 mmol) in 0.02 M DCM, AB-type monomer **(5)** (0.970 g, 3.54 mmol) was added slowly and solubilized. Finally, *tert*-butyl isocyanide (1.50 g, 18 mmol) was added dropwise. After stirring for three days at room temperature, the polymer was precipitated from ice-cold diethyl ether and Passerini diblock copolymer **P1** was obtained as a white solid (1.152 g, 87%) and characterized by ^{1}H NMR, ^{13}C NMR and SEC in THF.

^{1}H NMR (400 MHz, $CDCl_3$) δ/ppm: δ 6.10 (m, 25H, NH_O), 5.06 (m, 26H, CH_i), 4.21 (m, 2H, CH_d), 3.78–3.66 (m, 176 H, CH_b), 3.38 (s, 3H, CH_a), 3.19–3.15 (m, 2H, CH_g), 2.85–2.76 (m, 54H, CH_{fhv}), 2.70 (t, J = 6.6 Hz, 48H, CH_Z), 2.57 (t, J = 6.6 Hz, 48H, CH_W), 1.94–1.76 (m, 52H, CH_{rs}), 1.65–1.51 (m, 51H, CH_u), 1.35–1.19 (m, 598H, CH_{qt}).

^{13}C NMR (101 MHz, $CDCl_3$) δ 170.73 C_e, 169.11 C_m, 74.70 C_i, 70.7–70.6 C_{bd}, 51.61 C_a, 51.55 C_p, 34.89 C_f, 32.27 C_h, 31.92 C_v, 29.62 C_t, 29.55 C_t, 29.45 C_t, 29.30 C_q, 28.9 7 C_s, 28.82 C_u, 27.18 C_s, 24.82 C_g.

$M_{n,THEO}$: 11 300 g mol^{-1}. $M_{n,SEC(THF)}$: 16 300 g mol^{-1}, $Đ$ 1.55 (polystyrene equivalent values).

Synthesis of P2 – Passerini-3CR polymerization

The synthesis was adapted from a previous route.[13] To a vigorously stirred solution of *O*-methyl-*O*′-succinyl polyethylene glycol 2 kDa (0.076 g, 0.036 mmol) in DCM 0.02 M, AB bifunctional monomer **(5)** (0.051 g, 0.18 mmol) was added

slowly and solubilized. Finally, but-3-en-1-yl 12-isocyanododecanoate **(4)** (0.260 g, 0.93 mmol) was added dropwise. After stirring for three days at room temperature, the polymer was precipitated from ice-cold diethyl ether and Passerini diblock copolymer **P2** was obtained as a white solid (0.150 g, 0.030 mmol, yield 83%) and was characterized by ^{1}H NMR, FT-IR and SEC in THF.

^{1}H NMR (400 MHz, $CDCl_3$) δ 6.54(s, 5H, H_k), 5.83–5.74 (m, 5H, H_t), 4.28–4.24 (m, 5H, H_i), 4.15–4.10 (m, 10H, H_r), 3.71–3.64 (s, 126H, H_b), 3.38 (s, 3H, H_a), 3.26–3.16 (s, 10H, H_n), 2.93–2.53 (m, 29H, H_{zwfg}), 2.40–2.37 (m, 10H, H_s), 2.31–2.25 (m, 10H, H_p), 1.90–1.47 (m, 85H, H_v), 1.37–1.19 (s, 116H, H_o).

^{13}C NMR (101 MHz, CDCl3) δ173.97 C_q, 173.67 C_z, 170.76 C_m, 169.81 C_h, 134.17 C_t, 117.26 C_u, 74.17 C_i, 72.06 C_d, 70.69 C_b, 63.38 C_r, 59.16 C_a, 39.39 C_n, 34.73 C_p, 34.45 C_v, 33.24 C_w, 31.99 C_v, 29.65–29.56 C_{vy}, 29.36 C_o, 29.27 C_f, 29.04 C_g, 27.36 C_o, 27.02 C_o, 25.11 C_v.

P2 oxidation to P3 *via* ozonolysis

P2 (0.100 g, 0.020 mmol) was dissolved in DCM (25 mL). The solution was cooled to −78 °C with stirring and then the flask was attached to an ozone generator equipped with an oxygen cylinder. Molecular oxygen was bubbled through the solution for 5 minutes, then the ozone generator was switched on, and the ozone/oxygen mixture was bubbled through the solution maintaining −78 °C for 1 h. After a persistent metallic blue color developed, the ozone generator was switched off, and molecular oxygen was bubbled through the reaction mixture for 5 minutes. Dimethyl sulfide (1 mL, 13 mmol) was then added over a 20 minutes period with stirring at −78 °C, turning the mixture deep yellow. The resulting mixture was stirred at −78 °C for a further 1 h, then was allowed to warm to room temperature and left stirring for a further 1 h. The reaction mixture was dried under vacuum and diluted with 3 mL of acetone. The Passerini diblock copolymer **P3** was collected by precipitation in cold diethyl ether and obtained as a white solid (0.095 g, 0.018 mmol, yield 93%) characterized by ^{1}H NMR, FT-IR and SEC in THF.

^{1}H NMR (400 MHz, $CDCl_3$) δ 9.78 (s, 5H, Ht), 6.72–6.53 (s, 5H, H_k), 5.23–5.15 (m, 5H, H_i), 4.43–4.40 (m, 10H, H_r), 4.26–4.20 (m, 2H, H_d), 3.68–3.59 (s, 172H, H_b), 3.38 (s, 3H, H_a), 3.28–3.16 (m, 10H, H_j), 3.04–2.96 (m, 10H, H_n), 2.78–2.75 (m, 10H, H_s), 2.63–2.62 (m, 10H, H_w), 2.31–2.26 (m, 10H, H_p), 2.09–1.79 (m, 14H, H_{yfg}), 1.42–1.19 (m, 135H, H_{vo}).

^{13}C NMR (101 MHz, CDCl3) δ = 211.41 C_u, 175.81 C_q, 173.81 C_z, 173.72 C_m, 165.70 C_h, 72.06 C_i, 70.90 C_d, 70.69 C_b, 62.78 C_r, 59.38 C_a, 54.23 C_j, 53.89 C_y, 39.58 C_n, 34.31 C_p, 34.14 C_v, 32.73 C_w, 31.60 C_v, 29.53–29.02 C_{vyofg}, 26.91 C_o, 26.86 C_o, 24.88 C_v.

Synthesis of P1-Cy5 and P3-Cy5

P1 (18.34 mg, 1.53 μmol) was solubilized in 0.5 mL of dry dimethylformamide (DMF). *N*,*N*′-Dicyclohexylcarbodiimide (0.78 mg, 3.82 μmol) and *N*-hydroxysuccinimide (0.26 mg, 2.29 μmol) were added to the mixture. The reaction mixture was stirred at room temperature for 12 h and then **Cy5** amine (1 mg, 1.53 μmol) was dissolved in 0.1 mL of dry DMF and subsequently added. The reaction was left for 72 h. The crude mixture was diluted with 0.6 mL of acetone and the polymer was collected by precipitation into cold diethyl ether. The powder was dried, the polymer was solubilized in 0.5 mL of THF, diluted with 1 mL deionized water and then it was directly dialyzed against deionized water for 48 h (3.5 kDa cut-off, ThermoScientific). **P1-Cy5** was collected after freeze drying (17.5 mg, yield 95.41%). The **Cy5** conjugation yield was determined by UV/Vis spectroscopy. The **Cy5** conjugation yield was calculated by absorbance spectroscopy: **P1-Cy5**-labelled polymer was solubilized in 40 μL of DMF and diluted with water to 400 μL of water, the absorbance was recorded at 646 nm with a Tecan Spark 10M plate reader in a 96 well plate. A solution of water/10% DMF was used as a blank. The **Cy5** molar content was quantified by using the calibration curve in Fig. S12 (ESI†) and the **Cy5 :** polymer molar ratio was calculated. The **Cy5 : P1** polymer molar ratio was 1 : 2 and the conjugation yield was found to be 33%.

P3 (5 mg, 0.97 μmol) was solubilized in the minimum amount of dry DMF. *N*,*N*′-Dicyclohexylcarbodiimide (0.5 mg, 2.42 μmol) and *N*-Hydroxysuccinimide (0.167 mg, 1.45 μmol) were added. The reaction mixture was stirred at room temperature for 12 h and then **Cy5** amine (0.5 mg, 0.76 μmol) was solubilized in the minimum amount of dry DMF and then added. The reaction was left for 72 h. The crude was diluted with acetone and the polymer was collected by precipitation in cold diethyl ether. The powder was dried, the polymer was solubilized in 0.5 mL of THF, diluted with 1 mL DI water and then it was directly dialyzed against DI water for 48 h (3.5 kDa cut-off, ThermoScientific). **P3-Cy5**-labelled polymer was collected after freeze drying (4.9 mg; yield 98%). The **Cy5** conjugation yield was calculated by absorbance spectroscopy: **P3-Cy5**-labelled polymer was solubilized in 40 μL of DMF and diluted with water to 400 μL of water, the absorbance was recorded at 646 nm with Tecan Spark 10M plate reader in a 96 well plate. A solution of water 10% DMF was used as blank. The **Cy5** molar content was quantified by using the calibration curve in Fig. S12 (ESI†) and the **Cy5:**polymer molar ratio was calculated. Approximately 8% of the polymer chains were found to be functionalized with a **Cy5** molecule through amidation leading to 3.53 ± 0.05 wt% and 10% of conjugation yield.

Synthesis of P4-Dox

The synthesis was adapted from a published route.[25] Doxorubicin-HCl (0.128 g, 0.02 mmol) and triethylamine (0.04 g, 0.04 mmol) were solubilized in 0.2 mL of dimethyl sulfoxide (DMSO) and added to a solution of **P3** (0.05 g, 0.009 mmol) in 0.2 mL of DMSO under stirring for 7 h at room temperature. The crude was diluted with acetone and precipitated in cold diethyl ether. The powder was dried, solubilized in chloroform and the polymer-doxorubicin conjugate **P4-Dox** (0.022 g, 0.002 mmol, 32% yield) was collected and dried under vacuum after size exclusion purification through Sephadex LH20.

^{13}C NMR (126 MHz, $CDCl_3$) δ 216.64 C_o, 186.18 C_p, 173.78 C_k, 173.21 C_k, 172.21 C_k, 171.42 C_k, 170.18 C_f, 170.08 C_f, 169.77 C_c, 156.00 C_m, 144.66 C_n, 127.41 C_n, 114.53 C_n, 113.66 C_n, 81.04 C_u, 75.31 C_u, 74.48 C_e, 69.04–65.98 C_b, 64.31 C_t, 61.82 C_r, 59.76

C_r, 59.19 C_a, 53.88 C_w, 40.99 C_s, 34.29 C_z, 31.94 C_u, 31.83 C_v, 31.71 C_v, 29.70 C_v, 29.38 C_q, 29.23 C_q, 28.61 C_v, 28.47 C_v, 28.23 C_v, 27.11 C_v, 26.81 C_v, 24.90 C_v, 24.75 C_v, 22.82 C_v, 22.55 C_v, 22.00 C_v, 15.45 C_j, 15.39 C_v, 8.80 C_v.

Formulation and characterization

Transmission electron microscopy (TEM) characterisation. The morphology of Passerini polymersomes and nanoparticles was examined by transmission electron microscopy (TEM). An aliquot (13 μL) of polymersomes in PBS (5 mg mL^{-1}) were deposited onto a Formvar/Carbon film 200 mesh copper grid (EM Resolutions.com) for one minute and then the grid was blotted with filter paper. The sample was stained by depositing onto the grid 13 μL of uranyl acetate 2% solution in water for 30 s, then the grid was blotted with filter paper and dried in air.

P1 and P1-Cy5 empty polymersomes formulation. Passerini diblock copolymer **P1** polymersomes were prepared by nanoprecipitation. **P1** was dissolved at 5 mg mL^{-1} concentration in THF and added to PBS at 150 mM pH 7.4 while stirring, using a syringe pump (flow rate: 0.4 mL min^{-1}) at 1 : 1 volume ratio. The organic solvent was let evaporating overnight in the fume hood and the polymersomes size (*z*-average diameter) was measured using NanoZS equipment (Malvern, UK) at 25 °C (DLS).

P1-Dox polymersomes formulation. The formulation of doxorubicin-loaded **P1-Dox** polymersomes was performed by adapting the remote pH transmembrane gradient method from the literature.[26,27] The Passerini diblock copolymer **P1** 5 mg mL^{-1} in THF was added to citrate buffer 150 mM pH 4 while stirring, using a syringe pump (flow rate: 0.4 mL min^{-1}) at 1 : 1 volume ratio. The organic solvent was allowed to evaporate overnight under stirring. Then, the pH of the formulation was raised to 7.4 by adding ~2 μL of NaOH 2 M. Doxorubicin hydrochloride solution in DMSO was added to the aqueous polymersomes solution (5 mg **P1** : 2 mg doxorubicin) leading to 30% v/v DMSO/PBS solution. Finally, the pH was raised to 8.2 by adding ~0.5 μL of NaOH 2 M leading to a pH gradient of Δ = 4.2. The solution was left under stirring for 3 days in the dark. **P1-Dox** was directly dialyzed against PBS 150 mM for 24 h (3.5 kDa cut-off, ThermoScientific). The particle size (*z*-average diameter) was measured as reported above.

P3-Cy5 and P4-Dox nanoparticles formulation. **P3-Cy5** or **P4-Dox** was dissolved at 5 mg mL^{-1} concentration in DMSO and added to PBS pH 7.4 150 mM while stirring, using a syringe pump (flow rate: 0.4 mL min^{-1}) leading to a solution 1 mg mL^{-1}; at 2 : 8 volume ratio. The organic solvent was removed by dialysis against PBS 150 mM for 24 h (3.5 kDa cut-off, ThermoScientific). The size (*z*-average diameter) was measured using NanoZS equipment (Malvern, UK) at 25 °C (DLS).

P1-Dox and P4-Dox polymersomes drug loading and encapsulation efficiency. Doxorubicin loading, encapsulation efficiency and doxorubicin content in the sterilized *in vitro* **P1-Dox** and **P4-Dox** formulations were determined by mixing 0.1 mL of formulation with 0.1 mL of trifluoroacetic acid for 5 h under stirring. The solution was then filtered through 0.22 μm filter (PVDF, 4MM, Chromacol4, ThermoFisher). Doxorubicin was quantified by HPLC on a Shimadzu apparatus equipped with a LC-10A Dvp pump, a SIL-10A Dvp auto-injector, a SPD-10 Avp UV–Vis detector, a RF-10A_{XL} fluorescence detector and a C-R6 integrator. LC solution software was used to analyze the chromatograms. The analysis was performed on an ACE Excel 5 super C18 HICHROM 5 μm, C18 column (250 × 4.6 mm, 100 Å – Hichrom, UK). The optimized mobile phase consisted of PBS 10 mM pH 6[28] (A) and acetonitrile HPLC grade (B). The mobile phase gradient program (A/B) was: 80 : 20 (t = 5 min), 40 : 60 (t = 20 min), 80 : 20 (t = 22 min) and was applied over 30 min at a flow rate of 1 mL min^{-1}. The fluorescence excitation and emission wavelengths were 485 and 590 nm respectively, the UV detector was set at 485 nm. The injection volume was 10 μL. The analysis was performed in triplicate.

The drug loading and encapsulation efficiency were calculated using the following equations:

$$\text{Drug loading } (\%) = \frac{\text{Weight of loaded drug}}{\text{Total weight of polymersomes}} \times 100 \quad (1)$$

$$\text{Drug encapsulation } \%\ (\text{w/w}) = \frac{\text{Total amount of drug} - \text{unloaded drug}}{\text{Total amount of drug}} \times 100 \quad (2)$$

P1-Dox and P4-Dox *In Vitro* drug release

Drug release studies were performed *in vitro* in PBS at 150 mM at pH 7.4 (blood pH)[29] and sodium acetate buffer at 150 mM pH 5.0 containing 0.15 M NaCl[30] (endosomal pH).[31,32] A sample of 250 μL of **P1-Dox** or **P4-Dox** formulation was diluted to 500 μL with PBS or acetate buffer 150 mM and the pH was adjusted to 7.4 or 5. The solution was placed in a dialysis device (Slide-A-Lyzer™ mini dialysis device, 3.5 K MWCO, Thermo Scientific). The **P1-Dox** or **P4-Dox** solution was dialyzed against 1.7 mL of release media 150 mM at 37 °C and samples (0.75 mL) were taken at appropriate time points and replaced with 0.75 mL of fresh media to maintain sink conditions.[33] The doxorubicin content of these samples was quantified by Agilent UV-Vis Spectrometer referring to the calibration curves.

Calibration curves

Doxorubicin hydrochloride in DMSO 1 mg mL^{-1} was diluted with PBS 150 mM pH 7.4 leading to different concentrations. The procedure was repeated in triplicate, the samples were analysed by UV-Vis spectrophotometer and the absorbance at 500 nm was plotted against doxorubicin concentrations leading to the calibration curve reported. Doxorubicin hydrochloride 1 mg mL^{-1} in acetate buffer pH 5 150 mM was diluted with acetate buffer leading to different concentrations. The procedure was repeated in triplicate, the samples were analysed by UV-Vis spectrophotometer and the absorbance at 490 nm was plotted against doxorubicin concentrations leading to the calibration curve reported.

Cell culture

The TNBC cell line MDA-MB-231 was acquired from the American Type Culture Collection (Manassas, VA). MDA-MB-231 cells

were maintained in RPMI 1640 (Gibco BRL, USA) supplemented with 10% (v/v) FBS and 5% L-glutamine and incubated at 37 °C in 5% CO_2.

Effects of polymers on cellular metabolism

The CellTiter-Fluor cell viability assay was performed to determine the cytotoxicity of **P1** and **P3** copolymers against MDA-MB-231 cells following the protocol provided by the vendor (Promega, Madison WI).[24] Cells were treated for 48 h with different concentrations of **P1** and **P3** copolymers.

MDA-MB-231 cells were seeded into 96 well-plate at a density of 6×10^3 cells per well and incubated at 37 °C, 5% CO_2 for 24 h. Afterwards, cells were exposed to different concentrations of **P1** and **P3** copolymers (in complete media - sterilized under 254 nm UV light for 30 minutes) for 48 h. Negative controls were prepared by treating the cells with 1% Triton X. Cells were then washed three times with complete media and incubated at 37 °C, 5% CO_2 with a solution of media and CellTiter-Fluor Cell Viability Assay (1 : 1) for 1 h. 1 mg mL^{-1} solution of **P1** and **P3** copolymers in media was incubated with CellTiter-Fluor Cell in order to investigate any possible interactions. The fluorescence was then measured with Tecan Spark 10M ($400nm_{Ex}/505nm_{Em}$). Experiments were made in replicates, repeated in different days and the protease activity (mean% ± SD) was reported compared to the controls and calculated as mentioned in eqn (3).

$$\text{Protease activity} = \frac{\text{RFU sample} - \text{RFU negative control}}{\text{RFU positive control} - \text{RFU negative control}} \quad (3)$$

Preparation of 3D cancer cell spheroids

TNBC tumour spheroids were obtained using ultra-low attachment (ULA) 96-well round bottom plates (Corning, UK). MDA-MB-231 cells were seeded into ULA plates at a density of 4000 per well and cells were centrifuged at 200×g for 3 minutes after seeding to bring the cells closer together and aid in the formation of a single spheroid. Spheroids were then cultured for 4 days before final analysis or treatment.

Evaluation of internalisation of P1-Cy5 and P3-Cy5 nanoparticles by cancer cells

2D monolayer. MDA-MB-231 cells were seeded into 6-well plates at a density of 7.5×10^4 cells per well for 24 h in complete media at 37 °C in 5% CO_2. Cell culture media was replaced with the media containing **P1-Cy5** or **P3-Cy5** labelled nanoparticles 4h in the dark at 37 °C in 5% CO_2. Media was then removed and cells were washed with PBS for three times and then detached with 500 μL of TrypLE (1×) solution. Cells were centrifuged and resuspended in 500 μL of paraformaldehyde solution in PBS (4%) and then analysed by flow cytometry (Beckman Coulter FC 500). Generated data were analysed using Kaluza 1.5 software. Experiments were made in replicates and repeated over different days.

3D tumour TNBC spheroids. MDA-MB-231 cells were seeded into a ULA 96 well-plate at a density of 4000 per well and the spheroids were formed using the same procedure as previously reported.[21] The spheroids were then exposed to 1 μL of **P1-Cy5** or **P3-Cy5** labelled polymer of 25 μg mL^{-1} in the dark at 37 °C in 5% CO_2 for 16 h. The spheroids were disassembled and the cells of 18 wells were collected to make one flow cytometry sample. The pellet was collected by centrifugation, washed with PBS, centrifuged and finally resuspended in 500 μL of paraformaldehyde solution in PBS (4%). The samples were analysed by flow cytometry as previously mentioned.

Confocal microscopy

2D monolayer. MDA-MB-231 cells were cultured on micro slide 8-well chambers (Ibidi, Germany) at a density of 1×10^4 cells per well for 24 h in RPMI 1640 complete media at 37 °C in 5% CO_2 for 24 h.

Cells were exposed to 25 μg mL^{-1} **P1-Cy5** or **P3-Cy5** labelled nanoparticles in the dark at 37 °C in 5% CO_2 for 4 h. Following incubation, cells were washed with PBS three times, incubated with CellMask Green plasma membrane stain at the concentration of 1 μL mL^{-1} (100 μL) for 10 minutes in the dark at 37 °C in 5% CO_2 and washed with PBS three times. Cells were then incubated with Hoechst 33342 dye at concentration of 1 μg mL^{-1} (100 μL) for 30 minutes in the dark at room temperature and washed again with PBS (three times). Finally, cells were fixed with 4% formaldehyde (in PBS) for 10 min and again washed with PBS (three times). Cells were imaged with a Zeiss LSM 700 Confocal Laser Scanning Microscope. Zen 2.6 blue image Software was utilized for image processing.

3D tumor TNBC spheroids. MDA-MB-231 cells were seeded into a ULA 96 well-plate at a density of 4000 per well and the spheroids were formed using the same procedure as previously reported. The spheroids were then exposed to 1 μL of **P1-Cy5** or **P3-Cy5** labelled polymer of 25 μg mL^{-1} in the dark at 37 °C in 5% CO_2 for 16 h. Afterwards, the media was gradually removed and the spheroids were carefully washed with PBS three times. The spheroids were then stained with Hoechst 33342 dye at concentration of 1 μg mL^{-1} (50 μL) for 30 minutes in the dark at room temperature and washed again with PBS (three times). The spheroids were fixed with 4% formaldehyde (in PBS) for 10 min and again washed with PBS (three times). Cells were imaged as previously mentioned.

Results

In order to exemplify the strategy for drug delivery materials, we chose to design Passerini polymers with functionality to enable self-assembly into nanoparticles and polymersome structures, and with conjugation or encapsulation of doxorubicin for targeting TNBC. This is because doxorubicin is a standard treatment for TNBC, which is an aggressive subtype of breast cancer and the leading cause of cancer deaths. TNBC is characterized by the absence of human epidermal growth factor receptor 2 and the lack of progesterone and estrogen receptors.[20,21] TNBC affects young patients, has high metastatic potential and poor clinical outcomes.[22] Only the 30–40% of the

chemotherapy-treated patients in early stage TNBC show positive pathological responses.[23]

The synthesis schemes are shown in Scheme 1. The Passerini diblock copolymers were synthesised in one-pot by reacting *O*-methyl-*O*′-succinyl polyethylene glycol 2 kDa (mPEG-COOH) as an irreversible chain transfer agent in a reaction involving AB-type monomer (**5**)[34] and an excess of the isocyanide opportunely functionalized at the R group (Scheme 1A). The polymersome forming copolymer **P1** was obtained in high yield (87%), with SEC data indicating a molar mass (M_n ~ 16 000 g mol^{-1}) and a molar mass distribution of $Đ$ = 1.55. The molar mass by NMR was lower (~11 000 g mol^{-1}), and the difference between this value and that from SEC may have been due to the different relaxation times, and hence measured integrals, for protons in the PEG block compared to the poly(ester) blocks. For the doxorubicin-polymeric prodrugs (Scheme 1C), a diblock copolymer **P2** was obtained with high yield (83%) and high conversion of the AB monomer units. The alkene pendant groups of **P2** were oxidatively cleaved to aldehyde groups *via* ozonolysis (**P3**). The peak *t* in the ^{1}H NMR of the as-produced polymer (Fig. S9, ESI†) and the FT-IR spectra (Fig. S11, ESI†) showed complete conversion of the alkene groups and the concomitant oxidation of the thioether units into sulfones. Although the sulfone group is reducible and thus potentially biologically active, prior reports of polymers containing sulfones in their main chain have shown no acute adverse effects in cell lines.[24,35] The Passerini copolymer chemistry was then exploited by conjugating the dye **Cy5** *via* amidation to the carboxylic end-groups leading to the fluorescently labeled **P3-Cy5** (SI). Subsequently, the **P3** side-chain aldehyde groups were conjugated with doxorubicin *via* an imine bond, in order to enable intracellular drug release. The ^{1}H NMR spectrum of the polymer prodrug **P4-Dox** (Fig. S13, ESI†) showed complete conjugation of the drug due to the disappearance of the aldehyde protons, which was further confirmed by the imine signal at 1654 cm^{-1} in the FT-IR spectrum Fig. S11 (ESI†).

Nanoparticle formulations and TNBC cell culture studies

Polymers **P1** and **P4-Dox** were found to self-assemble readily in buffer solutions, with mean diameters of ~140 nm (**P1**) to ~20 nm for **P4-Dox**). The dye-labelled polymer **P1-Cy5** also self-assembled, but formed smaller particles (~90 nm) and with a higher size dispersity than the parent polymer. As apparent from Fig. 1, a distinct polymersome membrane could be observed in the TEM micrographs of **P1**, whereas for **P4-Dox**, with a lower hydrophobic content, more conventional kinetically-trapped nanoparticulate structures were formed.

The difference in self-assembly behaviour can be attributed to the different ratios of hydrophilic to hydrophobic blocks in the polymer structures. For **P1** the degree of hydrophobicity based on block content[13] was ~70% (see Scheme 1B) based on SEC-derived mass or ~55% based on NMR mass, whereas for **P4-Dox** the hydrophobic content was less than 30%. Accordingly, the packing parameters for **P1** chains were in the expected region for vesicle/polymersome formation,[36] whereas for **P4-Dox**, the hydrophilic : hydrophobic ratio indicated that more micellar-type structures should be formed. The overall diameters of the **P4-Dox** nanoparticles were larger than expected for 'pure' core-shell structures, in which the surface was only the PEG-layer and the core solely the hydrophobic regions, again in agreement with many prior studies of polymer nanoparticles.[21]

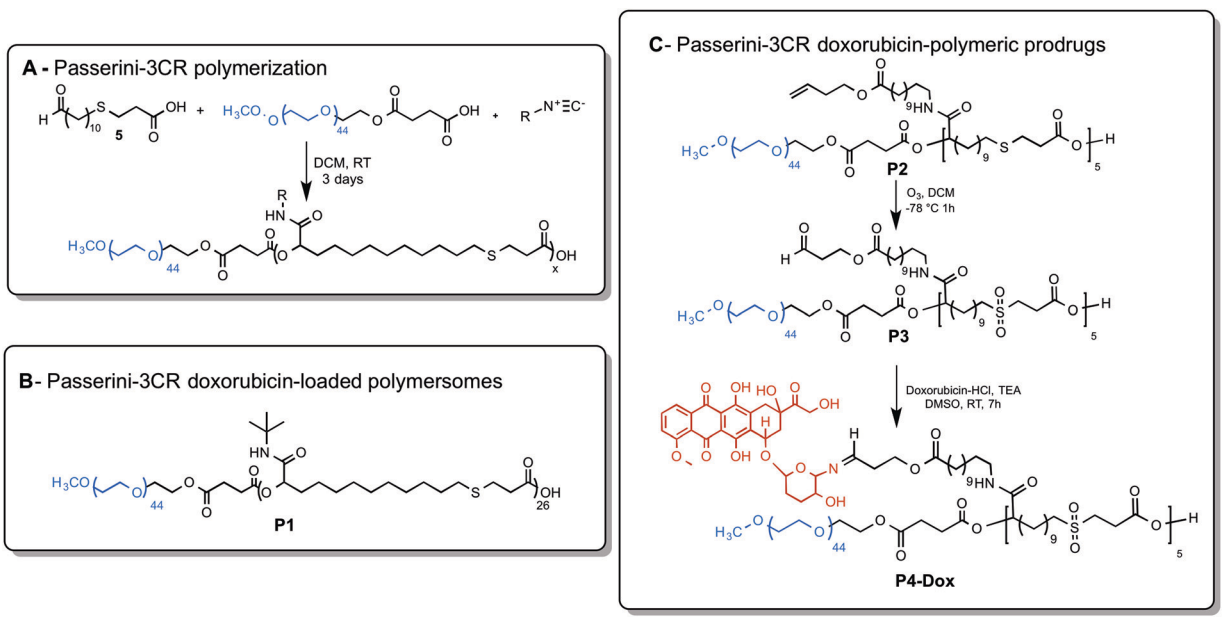

Scheme 1 (A) Passerini-3CR general polymerization reaction: mPEG-COOH was reacted with AB-type monomer and an excess of isocyanide properly functionalized (*R*). (B) **P1** Passerini copolymer structure for the assembling of polymersomes. (C) **P4-Dox** for Passerini doxorubicin-polymeric prodrug synthetic route. **P2** Passerini copolymer alkene groups were oxidatively cleaved into aldehydes (**P3**), which were finally conjugated through imine linker with doxorubicin (**P4-Dox**).

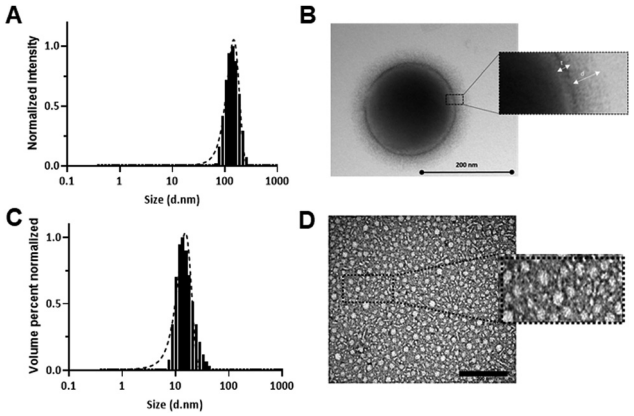

Fig. 1 Dynamic Light Scattering (DLS) and Transmission Electron Microscopy (TEM) of nanoparticles prepared from **P1** (A and B) and **P4-Dox** (C and D). Insets, magnified images to show polymersomes and nanoparticles for **P1** and **P4-Dox** respectively. Scale bars – 200 nm.

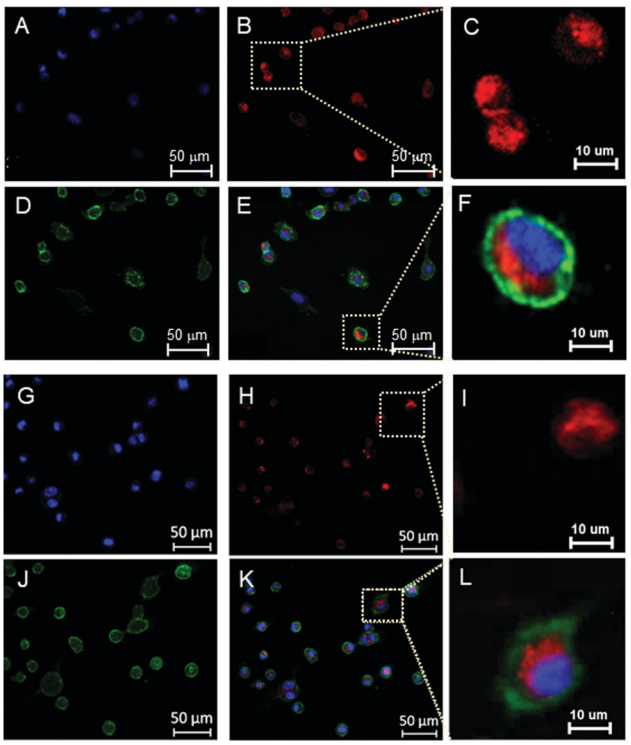

Fig. 2 Confocal micrographs show internalisation of nanoparticles prepared from **P1-Cy5** (A–F) and **P3-Cy5** (G–L) in MDA-MB-231 TNBC cells after 4 hours. Nuclei are stained blue (Hoechst 33342), membranes green (CellMask-Green) and polymers red (**Cy5**). Scale bars are 50 μm for full image and 10 μm for magnified regions.

Tagging of the polymers with an amino-functional **Cy5** label at the carboxyl terminus *via* NHS/DCC coupling allowed monitoring of their internalization in 2D monolayers and 3D spheroid cell cultures. MDA-MB-231 cells were chosen as a representative TNBC cell line, and entry of the polymers into the cells was evaluated by confocal microscopy and flow cytometry. Confocal images in 2D cultures of MDA-MB-231 cells (Fig. 2) showed that **P1-Cy5** and **P3-Cy5** nanoparticles were internalized by the cells.[31]

Transport of drug delivery carriers *in vivo* is known to correlate better with 3D cell cultures than with 2D monolayers, and thus the ability of the **Cy5** labelled formulations to permeate throughout 3D spheroids was assayed. In these experiments, imaging was carried out after the cells had grown together for 4 days, such that the resultant spheroids were dense and close packed. Following an incubation time for the polymers of 16 h, the dye-labelled polymers in the cells were imaged by confocal microscopy and quantified by flow cytometry.

As can be seen in Fig. 3A–F and as reported in the ESI† (Fig S29, S30), the nanoparticles penetrated deep into the spheroids and were efficiently internalized by the tumour cells. The uptake of the polymers was quantified by flow cytometry and found to be concentration-dependent (Fig. 3G and H). These data were in accord with our previous studies of polymer nanoparticle penetration into TNBC spheroids.[37,38]

Effects of polymers with/without doxorubicin in breast cells

Following the demonstration of cell entry for both formulations into TNBC cells we evaluated their efficacy in drug delivery assays. Initially, **P1** and **P3** copolymers were dosed at increasing levels in 2D monolayers of TNBC (MDA-MB-231). The **P1** polymers were well-tolerated up to 0.5 mg mL^{-1} whereas the **P3** polymers exhibited signs of toxicity at 100 μg mL^{-1}, which we attribute to the free aldehyde function in the latter (Fig. S23, ESI†). The **P1** empty polymersomes were then loaded with doxorubicin by adapting the remote transmembrane pH gradient method reported for the formulation of liposomes by Li *et al.*[26] The polymersomes were first assembled in 150 mM citrate buffer at pH 4 and then the pH gradient was created by adding 2 μL of NaOH 2M and raising the external pH to 7.4. Doxorubicin was dissolved in DMSO, which acted also to plasticise the polymer membrane, and added to the polymersomes aqueous solution leading to an overall 30% (v/v) and to increase the pH gradient from 3.43 to 4.2. As reported by Li *et al.*,[26] the protonated doxorubicin can aggregate with the citrate anions forming insoluble fibrous structures, which are in equilibrium with the soluble drug molecules. Therefore, doxorubicin was expected to permeate throughout the polymeric bilayer and be trapped in the vesicular core as citrate complexes. **P4-Dox** prodrug nanoparticles were formulated as the self-assembled micellar-like nanoparticles formed in aqueous buffer solutions. The doxorubicin loaded nanoparticle drug loading was calculated by HPLC with values for **P1-Dox** and **P4-Dox** found to be 16 ± 3 wt% and 36 ± 2 wt%, respectively. Interestingly, the polymer:drug molecular ratio for **P1-Dox** polymersomes was found to be higher (1 : 4) than that reported by Ahmed *et al.*[39] **P4-Dox** drug loading was found to be higher than for **P1-Dox** as expected for a polymeric-prodrug formulation.[32,40]

Preliminary microscopy assays (Fig. 4) indicated that free doxorubicin (Fig. 4A–D) rapidly entered MDA-MB-231 cells and reached the nucleus after 4 h, whereas **P4-Dox** polymers showed a different signal localization for doxorubicin (Fig. 4E–H). We therefore evaluated the release profiles for doxorubicin from

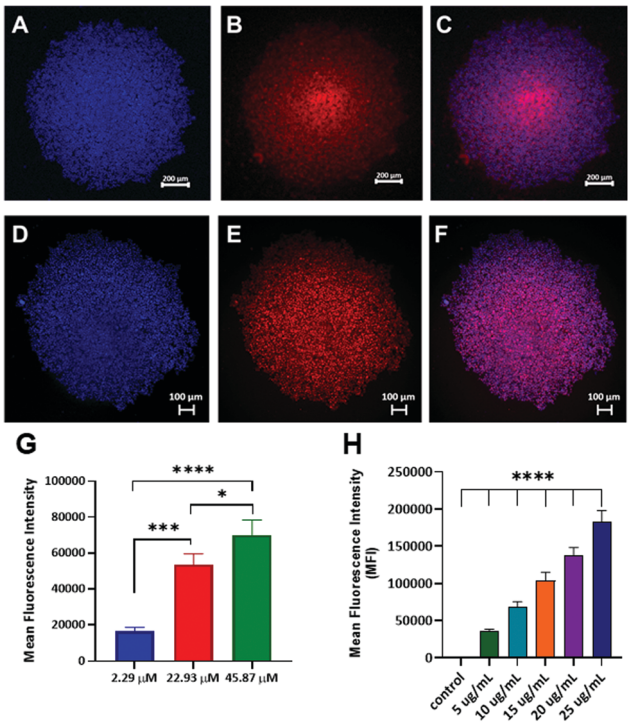

Fig. 3 (A–C, and D–F) Cellular uptake of **P1** and **P3-Cy5** fluorescently labelled nanoparticles in MDA-MB-231 cells assessed by confocal microscopy in 3D spheroids of MDA-MB-231 cells with nuclei stained with Hoechst 33342 (A and E), **P1-Cy5** polymersomes (B) and **P3-Cy5** nanoparticles (F), In (C and G) are, superimposition of A, B and E, F respectively. Scale bars 200 and 100 μm. In (G and H) are shown quantification by flow cytometry of the internalisation of polymers, reported as mean fluorescence intensity of **P1** and **P3-Cy5** nanoparticles, in MDA-MB-231 spheroids. (*$p < 0.05$, *t*-test).

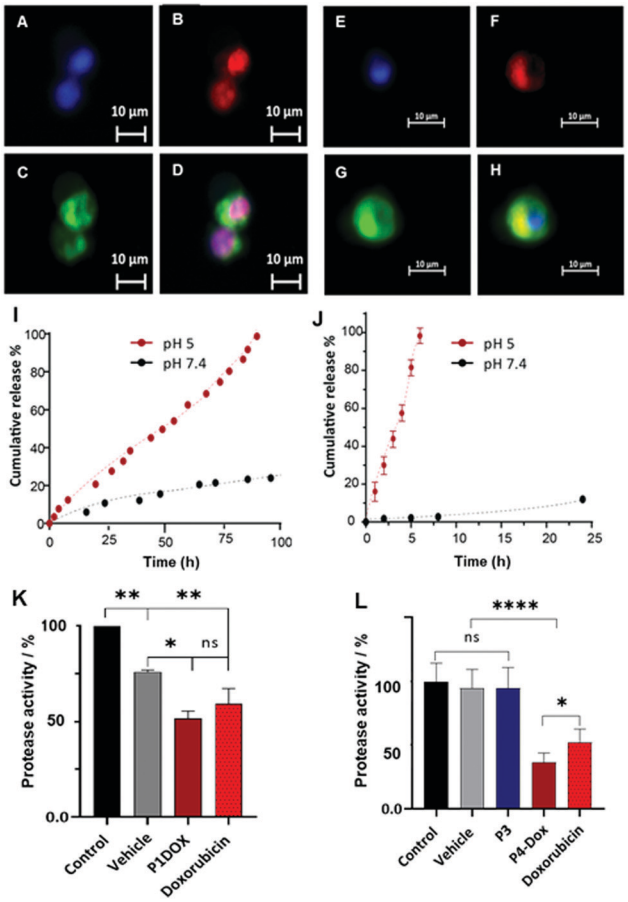

Fig. 4 Cellular uptake assessed by confocal microscopy of doxorubicin ((A and D) and **P4-Dox** (E–H) in MDA-MB-231 cells after 4 h incubation. (A and E) Nuclei stained with Hoechst 33342 (Ex 350 nm/Em 461 nm), (B) **P4-Dox** and (F) doxorubicin (Ex 480 nm/Em 590 nm), (C and G) Cell membrane stained with Cell MaskTM Deep Red plasma membrane stain (Ex 649 nm/Em 666 nm), (D and H) Merged image from the superimposition of A–C and E–G images. Scale bar 10 μm. In (I and J) are **P1-Dox** and **P4-Dox** drug release profiles at endolysosomal (pH 5) and blood (pH 7.4) mimicking pH conditions. In (K and L) are protease activity levels in MDA-MB 231 cells treated for 48 h with **P1-Dox** and **P4-Dox** nanoparticles respectively, free doxorubicin and vehicle (25% and 4% water in cell culture media respectively); In K are shown results of CellTiter-Glo 3D Cell Viability assays for free Doxorubicin at 0.4 nM and loaded doxorubicin in **P1-Dox** polymersomes also at 0.4 nM. Data are representative of three experiments (*$p < 0.05$, *t*-test). In (L) results show CellTiter-Fluo Cell Viability Assay of **P3** (0.09 nM), **P4-Dox** (at 0.49 nM doxorubicin equivalent) and free doxorubicin (0.49 nM) in 2D monolayers of MDA-MB-231 cells (*$p <$ 0.05, two-way ANOVA with Turkey's post-test).

the formulations over longer timescales and, as reported in Fig. 4(I and J), the drug cargoes in both **P1-Dox** and **P4-Dox** formulations were largely retained at ambient plasma pH,[29] but were released under pH conditions mimicking endo/lysosomal intracellular processing.[30–32] For the **P1-Dox** formulation, retention of the drug was expected to be reduced as the interior pH of the vesicles became acidic, and as shown in Fig. 4I, release of doxorubicin at pH 5 was faster than at pH 7.4. The overall time for full release was ~100 h, whereas only 20% of drug was released at pH 7.4 from the vesicles over the same time period. For the **P4-Dox** prodrug nanoparticles, which were designed to liberate doxorubicin through the pH-responsive hydrolysis of the imine-linker, complete release of drug occurred within 6 hours (Fig. 4J), with <5% of drug released from the same polymer at pH 7.4. The ~80% release of doxorubicin from **P4-Dox** under acidic conditions in 4 h (Fig. 4J) suggested that the drug should be liberated from the polymers if processed into digestive acidic intracellular compartments over this timescale.

We therefore decided to evaluate cytotoxicity of the polymers over a longer period in our efficacy assays. The data for 2D monolayers of MDA-MB-231 cells treated with **P1-Dox** polymersomes and **P4-Dox** prodrug nanoparticles in comparison to the free drug over 48 h is shown in Fig. 4(K and L). In these assays both **P1-Dox** nanoparticles and **P4-Dox** prodrug nanoparticles induced cell death, with **P4-Dox** showing a significantly enhanced cytotoxic effect compared to the free drug. While both formulations might have been expected to bypass membrane-bound transporters, which can act to pump free drug out of the cells, the greater efficacy of **P4-Dox** was most likely due to the greater overall release of doxorubicin over the 48 h period of incubation. The therapeutic potential of these materials will largely depend on their accumulation and retention time in tumours, and this may be problematic in TNBC as it is known that the EPR effect has limited relevance to many

human cancers. However, the fact that it was possible to introduce the self-assembly properties and drug conjugation links through Passerini-related chemistries, and that these in turn enabled tuning of the drug release profiles, suggests that the materials may have promise if their biodistribution can be optimised.

Overall, both the **P1-Dox** polymersomes and the **P4-Dox** formulations were found to exhibit slow release of the drug cargoes under normal physiological conditions, and to accelerate release under acidic conditions. We believe these results indicate that these chemistries could be important in developing 'platform' delivery formulations, built on a standard Passerini materials scaffold but with drug release performance modulated by control of assembly behaviour.

Conclusions

We have shown a simple and efficient route for tunable amphiphilic diblock copolymers synthesis *via* Passerini-3CR and their formulation into doxorubicin-loaded polymersomes and prodrug nanoparticles. The copolymers were found to be well-tolerated by TNBC cells in the absence of a drug cargo. The **Cy5** labelled formulations were internalized in 2D monolayers and 3D spheroids of TNBC and the uptake was found to be concentration-dependent. Additionally, **P1-Dox** and **P4-Dox** nanoparticles demonstrated pH-dependent drug release, with slow liberation of the cargo at plasma pH-values and accelerated release under pH conditions similar to those of intracellular compartments. **P4-Dox** prodrug nanoparticles showed both rapid drug release and improved toxicity against MDA-MB-231 cells, compared to **P1-Dox** and to the free drug. Our results suggest that the Passerini-3CR can provide a synthetically straightforward and flexible route to the synthesis of responsive drug delivery systems.

Conflicts of interest

There are no conflicts to declare.

Acknowledgements

This work was supported by the Engineering and Physical Sciences Research Council (Grant No. EP/N006615/1, EP/N03371X/1, EP/H005625/1, and EP/L013835/1). This work was also funded by the Royal Society (Wolfson Research Merit Award WM150086) to C.A. The authors thank the Nanoscale and Microscale Research Centre (nmRC) for providing access to instrumentation, Prof. Robert A. Stockman for providing access to the ozone generator, Douglas Crackett and Paul Cooling for expert technical assistance and Carol Turrill for outstanding administrative support.

References

1 W. Poon, B. R. Kingston, B. Ouyang, W. Ngo and W. C. W. Chan, *Nat. Nanotechnol.*, 2020, **15**, 819–829.
2 M. B. Ashford, R. M. England and N. Akhtar, *Adv. Ther.*, 2021, **4**, 2000285.
3 R. S. Riley, C. H. June, R. Langer and M. J. Mitchell, *Nat. Rev. Drug Discovery*, 2019, **18**, 175–196.
4 W. S. Saw, T. Anasamy, Y. Y. Foo, Y. C. Kwa, C. S. Kue, C. H. Yeong, L. V. Kiew, H. B. Lee and L. Y. Chung, *Adv. Ther.*, 2021, **4**, 2000206.
5 M. Machtakova, H. Therien-Aubin and K. Landfester, *Chem. Soc. Rev.*, 2022, **51**, 128–152, DOI: **10.1039/d1cs00686j**.
6 V. M. Weiss, H. Lucas, T. Mueller, P. Chytil, T. Etrych, T. Naolou, J. Kressler and K. Mäder, *Macromol. Biosci.*, 2018, 18.
7 J. Wang, S. Yuan, Y. Zhang, W. Wu, Y. Hu and X. Jiang, *Biomater. Sci.*, 2016, **4**, 1351–1360.
8 C. Oerlemans, W. Bult, M. Bos, G. Storm, J. F. W. Nijsen and W. E. Hennink, *Pharm. Res.*, 2010, **27**, 2569–2589.
9 H. Seyednejad, A. H. Ghassemi, C. F. van Nostrum, T. Vermonden and W. E. Hennink, *J. Controlled Release*, 2011, **152**, 168–176.
10 M. Passerini and L. Simone, *Gazz. Chim. Ital.*, 1921, **51**, 126–129.
11 B. Alkan, O. Daglar, S. Luleburgaz, B. Gungor, U. S. Gunay, G. Hizal, U. Tunca and H. Durmaz, *Polym. Chem.*, 2022, **13**, 258–266, DOI: **10.1039/D1PY01528A**.
12 L. Banfi, A. Basso, C. Lambruschini, L. Moni and R. Riva, *Chem. Sci.*, 2021, **12**, 15445–15472.
13 A. Travanut, P. F. Monteiro, S. Oelmann, S. M. Howdle, A. M. Grabowska, P. A. Clarke, A. A. Ritchie, M. A. R. Meier and C. Alexander, *Macromol. Rapid Commun.*, 2021, **42**, e2000321.
14 M. Meier, *Green Chem.*, 2014, **16**, 1672.
15 S. C. Solleder and M. A. R. Meier, *Angew. Chem., Int. Ed.*, 2014, **53**, 711–714.
16 M. Zhao, N. Liu, R.-H. Zhao, P.-F. Zhang, S.-N. Li, Y. Yue and K.-L. Deng, *ACS Appl. Bio Mater.*, 2019, **2**, 1714–1723.
17 B. T. Tuten, L. De Keer, S. Wiedbrauk, P. H. M. Van Steenberge, D. R. D'Hooge and C. Barner-Kowollik, *Angew. Chem., Int. Ed.*, 2019, **58**, 5672–5676.
18 Y.-Z. Wang, X.-X. Deng, L. Li, Z.-L. Li, F.-S. Du and Z.-C. Li, *Polym. Chem.*, 2013, **4**, 444–448.
19 F. Bray, J. Ferlay, I. Soerjomataram, R. L. Siegel, L. A. Torre and A. Jemal, *Ca-Cancer J. Clin.*, 2018, **68**, 394–424.
20 F. C. Geyer, F. Pareja, B. Weigelt, E. Rakha, I. O. Ellis, S. J. Schnitt and J. S. Reis-Filho, *Am. J. Pathol.*, 2017, **187**, 2139–2151.
21 P. F. Monteiro, M. Gulfam, C. J. Monteiro, A. Travanut, T. F. Abelha, A. K. Pearce, C. Jerome, A. M. Grabowska, P. A. Clarke, H. M. Collins, D. M. Heery, P. Gershkovich and C. Alexander, *J. Controlled Release*, 2020, **323**, 549–564.
22 R. Dent, M. Trudeau, K. I. Pritchard, W. M. Hanna, H. K. Kahn, C. A. Sawka, L. A. Lickley, E. Rawlinson, P. Sun and S. A. Narod, *Clin. Cancer Res.*, 2007, **13**, 4429.
23 G. Bianchini, J. M. Balko, I. A. Mayer, M. E. Sanders and L. Gianni, *Nat. Rev. Clin. Oncol.*, 2016, **13**, 674–690.
24 S. Oelmann, A. Travanut, D. Barther, M. Romero, S. M. Howdle, C. Alexander and M. A. R. Meier, *Biomacromolecules*, 2019, **20**, 90–101.
25 N. Xiao, H. Liang and J. Lu, *Soft Matter*, 2011, **7**, 10834–10840.
26 X. Li, D. J. Hirsh, D. Cabral-Lilly, A. Zirkel, S. M. Gruner, A. S. Janoff and W. R. Perkins, *Biochim. Biophys. Acta, Biomembr.*, 1998, **1415**, 23–40.

27 A. Choucair, P. Lim Soo and A. Eisenberg, *Langmuir*, 2005, **21**, 9308–9313.
28 R. R. Larson, M. B. Khazaeli and H. K. Dillon, *Appl. Occup. Environ. Hyg.*, 2003, **18**, 109–119.
29 J. A. Anderson, S. Lamichhane, T. Remund, P. Kelly and G. Mani, *Acta Biomater.*, 2016, **29**, 333–351.
30 V. Knorr, V. Russ, L. Allmendinger, M. Ogris and E. Wagner, *Bioconjugate Chem.*, 2008, **19**, 1625–1634.
31 C. Battistella and H.-A. Klok, *Macromol. Biosci.*, 2017, **17**, 1700022.
32 Y. Zhang, C. Yang, W. Wang, J. Liu, Q. Liu, F. Huang, L. Chu, H. Gao, C. Li, D. Kong, Q. Liu and J. Liu, *Sci. Rep.*, 2016, 6.
33 M. Gulfam, T. Matini, P. F. Monteiro, R. Riva, H. Collins, K. Spriggs, S. M. Howdle, C. Jerome and C. Alexander, *Biomater. Sci.*, 2017, **5**, 532–550.
34 S. Oelmann, S. C. Solleder and M. A. R. Meier, *Polym. Chem.*, 2016, **7**, 1857–1860.
35 D. Jeanmaire, J. Laliturai, A. Almalik, P. Carampin, D. A. Richard, E. Lallana, R. Evans, R. E. P. Winpenny and N. Tirelli, *Polym. Chem.*, 2014, **5**, 1393–1404.
36 T. P. Smart, O. O. Mykhaylyk, A. J. Ryan and G. Battaglia, *Soft Matter*, 2009, **5**, 3607–3610.
37 V. Taresco, T. F. Abelha, R. J. Cavanagh, C. E. Vasey, A. B. Anane-Adjei, A. K. Pearce, P. F. Monteiro, K. A. Spriggs, P. Clarke, A. Ritchie, S. Martin, R. Rahman, A. M. Grabowska, M. B. Ashford and C. Alexander, *Adv. Ther.*, 2020, 4.
38 H. Lu, R. H. Utama, U. Kitiyotsawat, K. Babiuch, Y. Jiang and M. H. Stenzel, *Biomater. Sci.*, 2015, **3**, 1085–1095.
39 F. Ahmed, R. I. Pakunlu, G. Srinivas, A. Brannan, F. Bates, M. L. Klein, T. Minko and D. E. Discher, *Mol. Pharmaceutics*, 2006, **3**, 340–350.
40 Y. Bae, N. Nishiyama, S. Fukushima, H. Koyama, M. Yasuhiro and K. Kataoka, *Bioconjugate Chem.*, 2005, **16**, 122–130.